Motor unit filter prelearning strategies for decomposition of compound muscle action potentials in high-density surface electromyograms*

A. Holobar, *Member, IEEE,* A. Frančič, *Student Member, IEEE*

***Abstract*— We analyze the efficiency of motor unit (MU) filter prelearning from high-density surface electromyographic (HDEMG) recordings of voluntary muscle contractions in the identification of the motor unit firing patterns during elicited muscle contractions. Motor unit filters are assessed from 10 s long low level isometric voluntary contractions by gradient-based optimization of three different cost functions and then applied to synthetic HDEMG recordings of elicited muscle contractions with dispersion of motor unit firings ranging from 13 ms to 1 ms. We demonstrate that the number of identified MUs and the precision of MU identification depend significantly on the selected cost function. Regardless the selected cost function and MU synchronization level, the median precision of motor unit identification in elicited contraction is ≥ 95 % and is comparable to the precision in voluntary contractions. On the other hand, median miss rate increases significantly from < 1 % to ~ 3 % with the tested level of MU synchronization.**

***Clinical Relevance*—The identification of MU firings from HDEMG in elicited muscle contractions provides a new tool for in vivo investigation of motor excitability in humans.**

I. Introduction

In the last two decades, motor unit (MU) identification from high-density surface electromyograms (HDEMG) gained a lot of scientific attention [2][4][6], providing a new tool for non-invasive in vivo investigation of neural codes during isometric voluntary muscle contractions. HDEMG decomposition methods are based on blind source separation approach, which first blindly estimates the MU filter and then applies it to the HDEMG signals to yield the MU spike train. In the last step, this spike train in segmented in order to separate the MU firings from the base line noise [9][10].

This decomposition approach highly efficiently combines the information from different HDEMG channels, calculating the optimal MU filter with predefined spatio-temporal support [10]. The MU filter can be optimized in calibration contractions and then applied directly to the newly recorded HDEMG in order to yield MU firings. This increases the robustness of MU identification as, in the calibration phase, MU filter can be optimized across several hundreds of MU firings and then applied to a very short HDEMG signals, such as the ones recorded during maximal or explosive muscle contractions [14]. In this way the statistical power of MU filter is efficiently transferred from the calibration to the exploitation phase (i.e. to new contraction).

Similarly, the MU filter optimization in calibration phase can be exploited for real-time decomposition of HDEMG signals. In this case, the MU filters are first estimated off-line and then applied in real time to the incoming HDEMG samples, enabling the online feedback on the activity of MUs to the measured subject [7].

In this study, we demonstrate that this prelearning of MU filters in the calibration phase can be utilized to identify MU firings also in the case of electrically elicited muscle contractions where the MU firings are highly synchronized. In particular, we test efficiency of different cost functions in gradient-based optimization of MU filters from HDEMG and their effects on the MU firing identification in the electrically elicited muscle contractions. As the methodology for experimental validation of MU identification in electrically elicited contraction is currently non-existing, at least to the beast of our knowledge, we base our analysis on the synthetic HDEMG signals with known MU firing patterns.

II. HDEMG signals and MU filter optimization

A. HDEMG data model

During short isometric muscle contractions, MU action potentials (MUAPs) can be assumed stationary and the HDEMG can be modeled as [9]:

$$\boldsymbol{y}(n) = \mathbf{H}\mathbf{t}(n) + \boldsymbol{\omega}(n), \tag{1}$$

where $\boldsymbol{y}(n) = [y_1(n) \dots y_1(n-F+1) \dots y_M(n-F+1)]^T$ contains blocks of F consecutive samples of M measurements (F is typically set between 5 and 15 [9]), $\boldsymbol{\omega}(n) = [\omega_1(n) \dots \omega_M(n-F+1)]^T$ is noise vector and

$$\mathbf{t}(n) = \left[t_1(n) \dots t_1(n-L-F+1) \dots t_J(n-L-F+1)\right]^T$$

with

$$t_j(n) = \sum_k \delta\left(n - \tau_j(k)\right), \quad j=1,\dots,J \tag{2}$$

comprises blocks of $L+F$ consecutive samples from J MU spike trains. In (2), $\delta(.)$ is a unit-sample pulse and $\tau_j(k)$ denotes the time of the k-th firing of the j-th MU.

The mixing matrix

* This study was supported by the Slovenian Research Agency (projects J2-1731 and L7-9421 and Programme funding P2-0041)

A. Holobar is with the Faculty of Electrical Engineering and Computer Science, University of Maribor, Maribor, Slovenia (corresponding author: phone +386-2220-7485; fax: +386-2220-7272; e-mail: ales.holobar@um.si).

A. Frančič is with the Faculty of Electrical Engineering and Computer Science, University of Maribor, Maribor, Slovenia (e-mail: aljaz.francic@um.si).

$$\mathbf{H} = \begin{bmatrix} \boldsymbol{H}_{11} \boldsymbol{H}_{12} \cdots \boldsymbol{H}_{1J} \\ \vdots \quad \vdots \quad \vdots \\ \boldsymbol{H}_{M1} \boldsymbol{H}_{M2} \cdots \boldsymbol{H}_{MJ} \end{bmatrix}, \tag{3}$$

contains MJ blocks of size $F \times (F+L)$, whereat block $\mathbf{H}_{ij}$ comprises temporarily shifted repetitions of L samples long MUAP from the j-th MU as detected by the i-th uptake electrode:

$$\mathbf{H}_{ij} = \begin{bmatrix} h_{ij}(1) & \dots & h_{ij}(L) & \dots & 0 \\ \vdots & \ddots & \ddots & \ddots & \vdots \\ 0 & \dots & h_{ij}(1) & \dots & h_{ij}(L) \end{bmatrix}. \tag{4}$$

B. MU filter optimization

Convolution Kernel Compensation (CKC) method initializes the filter of the j-th MU [9]:

$$\hat{\mathbf{f}}_j = \boldsymbol{y}(n_0)^T \mathbf{C}_{\boldsymbol{y}}^{-1}$$

where n_0 denotes randomly selected time moment with HDEMG activity above the noise level, $\mathbf{C}_{\boldsymbol{y}} = E(\boldsymbol{y}(n)\boldsymbol{y}^T(n))$ is the correlation matrix of HDEMG signals and $E(.)$ stands for mathematical expectation. Afterwards, CKC iterates the following equations [9]:

$$\hat{t}_j(n) = \hat{\mathbf{f}}_j^T \boldsymbol{y}(n) \tag{5}$$

$$\hat{\mathbf{f}}_j = \hat{\mathbf{f}}_j + \alpha E\left(g(\hat{t}_j(n))\boldsymbol{y}(n)\right)^T \mathbf{C}_{\boldsymbol{y}}^{-1} \tag{6}$$

$$\hat{\mathbf{f}}_j = \hat{\mathbf{f}}_j / \|\hat{\mathbf{f}}_j\| \tag{7}$$

where $\alpha < 1$ is a step size, $g(.)$ stands for element-wise non-linear weighting function, representing the derivative of the cost function that is being optimized by the gradient-based optimization. In order to avoid the determination of the step size α, Gauss-Newton optimization can be used in place of Eq. (6) [12]. In this study, the following weighting functions have been tested:

$$g_1(t) = \log(1 + \mathrm{t}^2) \tag{8}$$

$$g_2(t) = \tanh(\mathrm{t}^2) \tag{9}$$

$$g_3(t) = t \cdot e^{-\mathrm{t}^2/2} \tag{10}$$

Function g_1 was proposed in [11], whereas functions g_2 and g_3 are slightly modified from [12]. All these functions support robust MU identification (in the sense of base line noise and outliers), as they amplify the MU spikes on interval [0,1] whereat they limit (g_1 and g_2) or even penalize (g_3) larger MU spikes.

III. Simulations

We used cylindrical volume conductor model [3] to simulate HDEMG signals during voluntary and elicited contractions of biceps brachii muscle. For this purpose, 200 MUs were randomly distributed within the elliptical cross-section of size of 30 × 15 mm with the average density of 20 fibres/mm^2 [1]. Muscle fiber length was set to 130 mm with the innervation zone spread for 5 mm around the center of the fibers. The fat and the skin layers were 4 mm and 1 mm thick, respectively. The size of the MUs ranged from 24 to 2408 fibers and was exponentially distributed with many small and fewer big MUs [8]. MUAP conduction velocity was normally distributed with a mean of 4.0 ± 0.3 m/s.

MU firing patterns during the voluntary contraction were generated by the model described in [5], whereat we adapted the parameters to the properties of Biceps Brachii muscle. For these reasons, the MU recruitment thresholds ranged from 0 to 80 % of maximal excitation level, following the exponentially decreasing distribution [8]. The MU firing rate increased linearly with the simulated excitation level, from 8 pulses per second (pps) at the MU recruitment to 35 pps at maximal excitation [13]. The interspike interval was normally distributed with standard deviation set to 20 % of its mean value. The 10 s long voluntary contraction at 30 % of the maximal excitation level was simulated, resulting in 155 active MUs.

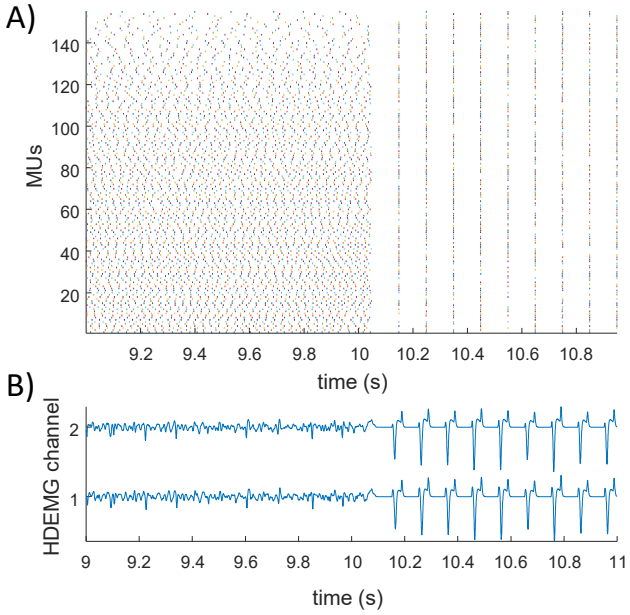

Figure 1. Generated MU firing patterns during the simulated elicited contraction (each colored dot is a MU firing) and corresponding HDEMG signals (Panel B). For clarity reasons only 2 channels of HDEMG signals are depicted.

The length of the elicited muscle contraction was also set to 10 s, with 10 simulated compound muscle action potentials (CMAPs) per second. For each CMAP, the MU firing times were normally distributed around the common mean value, with the standard deviation set to 13 ms, 7 ms, 3 ms, and 1 ms. This resulted in MU spike train synchronization (tolerance of 0.5 sample) of 10%, 20%, 40% and 80%, respectively. In order to facilitate the assessment of MU identification accuracy, 1/3 of randomly selected firings per MU were deleted during the elicited contraction. Firing patterns of voluntary and elicited muscle contraction were concatenated together, resulting in 20 s long muscle contractions. The example of generated firing pattern during simulated 80 % synchronization is depicted in Fig. 1.

HDEMG signals were detected by an array of 10 × 9 circular electrodes with diameter of 1 mm and the interelectrode

distance of 5 mm. Sampling frequency was 2048 Hz. The colored noise (bandwidth 20-500 Hz) was added to each HDEMG channel. The signal-to-noise ratio (SNR) was set to 30 dB. For each synchronization level, five different simulation runs were performed, with randomly distributed MUs within the simulated muscle tissue in each run.

A. Data analysis

The first 10 second of generated HDEMG signals (voluntary contraction) were decomposed by CKC method [9] with extension factor F=15 and the weighting function g(t) set to functions defined in Eqs. (8)-(10). For each weighting function, 50 decomposition runs were performed. Each identified MU spike train $\hat{t}_j(n)$ was segmented as proposed in [11]. Afterwards the Pulse-to-Noise Ratio (PNR) was calculated [11]:

$$PNR\left(\hat{t}_j(n)\right) = 10 \cdot \log\left(\frac{E\left(\hat{t}_j^2(n)\big|_{\hat{t}_j(n)=1}\right)}{E\left(\hat{t}_j^2(n)\big|_{\hat{t}_j(n)=0}\right)}\right), \qquad (11)$$

where $\hat{t}_j^2(n)\big|_{\hat{t}_j(n)=1}$ is the energy of segmented MU spikes (firings), whereas $\hat{t}_j^2(n)\big|_{\hat{t}_j(n)=0}$ is the energy of segmented baseline noise.

MU filters $\hat{\mathbf{f}}_j$ of MU that were identified with PNR ≥ 30 dB were saved and applied to the second 10 s of the HDEMG signals, identifying MU spike trains during the elicited muscle contraction. True positive (TP), false positive (FP) and false negative (FN) MU firings were identified with tolerance set to 0.5 ms. Afterwards, precision (Pr) and miss rate (MR) were calculated separately for voluntary and elicited contraction:

$$Pr = \frac{TP}{TP+FP}, \quad MR = \frac{FN}{FN+TP}, \qquad (12)$$

Non-parametric Kruskal-Wallis test and paired Wilcoxon rank sum test were used for further statistical analysis. When significant effect was observed, Bonferroni correction was applied with significance level set to $P < 0.05$

IV. Results

MU spike trains identified during the voluntary and elicited contraction are exemplified in Fig. 2. Weighting functions $g_1(t)$, $g_2(t)$ and $g_3(t)$ identified 8.8 ± 1.8 MUs, 9.7 ± 2.3 MUs and 5.2 ± 1.2 MUs, respectively. Average precisions and miss rates in voluntary and elicited contractions are depicted in Fig. 3 and Fig. 4, respectively. For clarity reasons, individual measured values are also depicted with red circles.

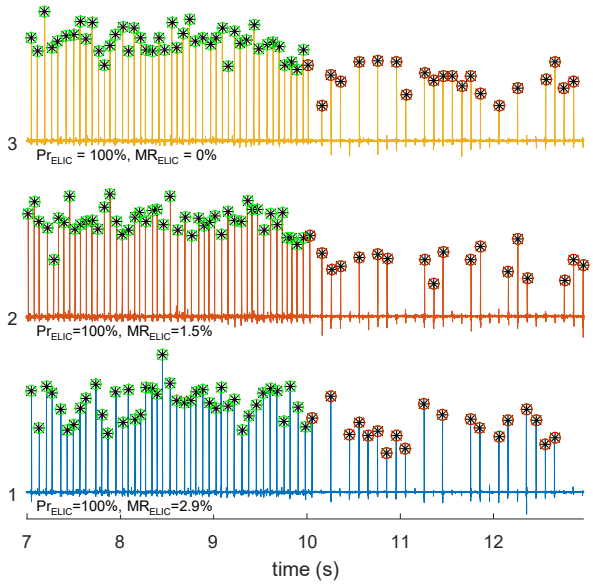

Figure 2. Identified MU spike trains during the voluntary and elicited muscle contraction (MU synchronization level of 10 %) for weighting function $g_1(t)$. TPs in voluntary (green circles) and elicited contraction (red circles) are also depicted, along with the simulated reference firings (black asterisk).

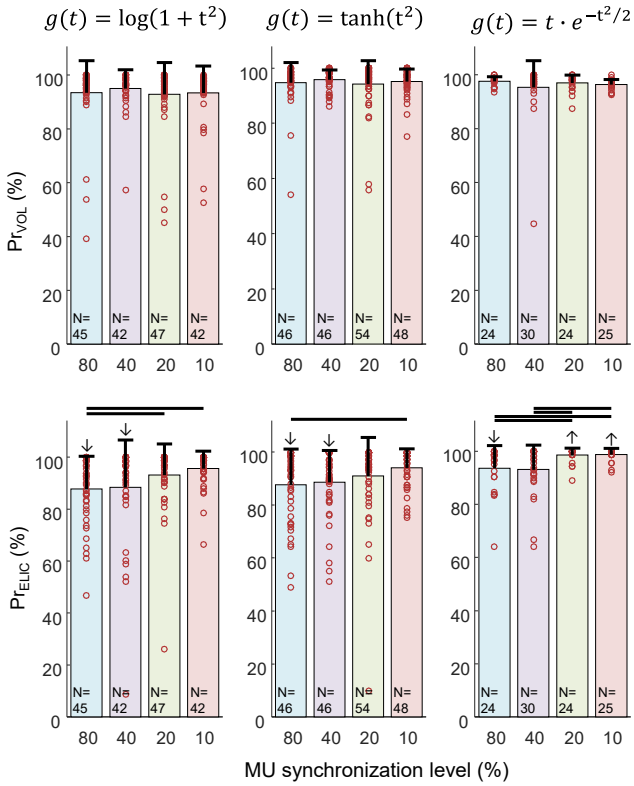

Figure 4. Precision (Pr) of MU firing identification during the voluntary (VOL) and elicited (ELIC) contraction as a function of weighting function *g*(*t*) and MU synchronization level: ↑ (↓) significantly higher (lower) than in voluntary contraction.

V. Discussion

In voluntary contraction $g_1(t)$, $g_2(t)$ and $g_3(t)$ weighing functions yielded MUs with precision of (mean ± SD [median ± IQR]) 93.1% ± 10.4% [96.2% ± 4.5%], 94.4%

± 6.4% [95.7% ± 3.9%] and 96.0% ± 5.7% [97% ± 2.7%], respectively. When averaged across all the simulated MU synchronization levels in elicited contractions, these figures decreased to 91.2% ± 13.3% [96.6% ± 11.6%], 90.4% ± 12.4% [94.3% ± 11.9%] and 95.9% ± 7.1% [98.5% ± 5.7%]. Regardless the weighting function, decrease in the precision was statistically significant for the highest two simulated synchronization levels (Fig. 3). At the same time, MU firing miss rates were 5.6% ± 14.1% [0.8% ± 2.5%], 4.5% ± 11.4% [0.8% ± 2.5%] and 1.5% ± 7.8% [0.4% ± 0.8%] in voluntary and 9.8% ± 13.0% [3% ± 12.4%], 10.3% ± 14.2% [4.4% ± 10.3%] and 5.0% ± 7.4% [2.9% ± 4.1%] in elicited contractions. Due to relatively large number of outliers, the median values of precisions and miss rates were largely different from the mean values. At 80% MU synchronization, the precision of MU identification by CKC was significantly lower in elicited than in voluntary contraction, regardless the tested weighting function. Similar decrease was also observed at 60% synchronization for $g_1(t)$ and $g_2(t)$ functions. On the other hand, the miss rate consistently increased in elicited contractions, regardless the weighting function used.

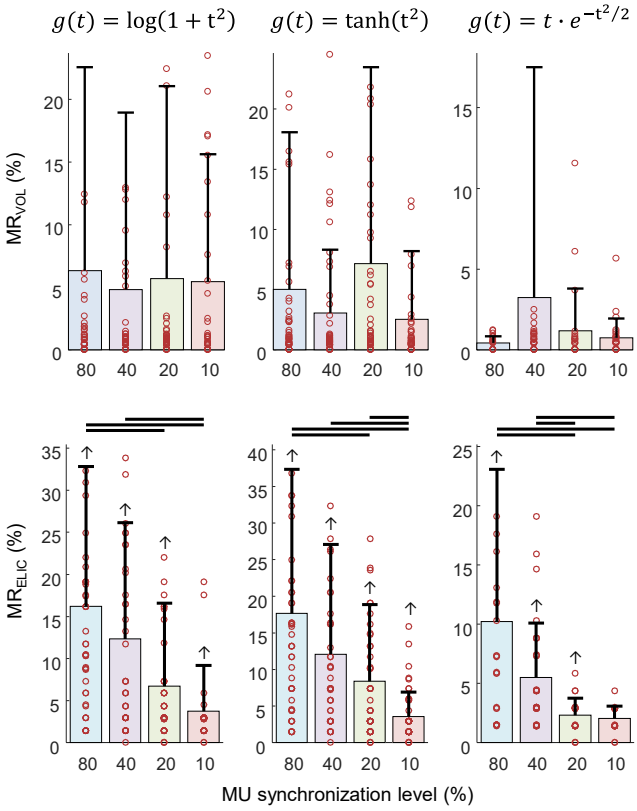

Figure 4. Miss rate (MR) of MU firing identification during voluntary (VOL) and elicited (ELIC) contraction as a function of weighting function $g(t)$ and MU synchronization level: ↑ significantly higher than in voluntary contraction.

Although demonstrating higher precision and lower miss rate, CKC with $g_3(t)$ weighting function identified significantly fewer MUs than CKC with $g_1(t)$ and $g_2(t)$ function (Fig. 3). Because the MU filters were identified from voluntary contraction, the number of identified MUs did not depend significantly on the synchronization level. Importantly, all the MUs identified in the voluntary contraction were successfully tracked also in the elicited contraction.

This study was limited to the simulated conditions as it is very difficult to derive the ground truth about MU firings in experimentally recorded elicited contractions. Furthermore, no stimulation artefact was simulated. Thus, the capability of MU filters to cope with the stimulation artefacts remains to be analysed. In the worst case scenario, stimulation artefact should be masked out, meaning that they must not overlap with the CMAPs. Finally, relatively small instrumental noise was simulated in this study, though the number of simulated MUs and, thus, the physiological noise was relatively large.

In conclusion, we tested the efficiency of different MU filter prelearning techniques in simulated cases of elicited muscle contractions and showed that the MU firings can be identified from CMAPs in HDEMG signals.

REFERENCES

[1] J. B. Armstrong, P. K. Rose, S. Vanner, G. J. Bakker, and F. J. Richmond, "Compartmentalization of motor units in the cat neck muscle, biventer cervicis," *J. Neurophysiol.*, vol. 60, no. 1, pp. 30–45, Jul. 1988.

[2] M. Chen and P. Zhou, "A Novel Framework Based on FastICA for High Density Surface EMG Decomposition," *IEEE Trans. Neural Syst. Rehabil. Eng.*, vol. 24, no. 1, pp. 117–127, Jan. 2016.

[3] D. Farina, L. Mesin, S. Martina, and R. Merletti, "A surface EMG generation model with multilayer cylindrical description of the volume conductor," *IEEE Trans. Biomed. Eng.*, vol. 51, no. 3, pp. 415–426, Mar. 2004.

[4] D. Farina and A. Holobar, "Characterization of Human Motor Units From Surface EMG Decomposition," *Proc. IEEE*, vol. 104, no. 2, pp. 353–373, Feb. 2016.

[5] A. J. Fuglevand, D. A.Winter, and A. E.Patla, "Models of recruitment and rate coding organization in motor-unit pools," *J. Neurophysiol.*, vol. 70, no. 6, pp. 2470–2488, Dec. 1993.

[6] J. A. Gallego, J. L. Dideriksen, A. Holobar, J. Ibáñez, J. L. Pons, E. D. Louis, E. Rocon, and D. Farina, "Influence of common synaptic input to motor neurons on the neural drive to muscle in essential tremor," *J. Neurophysiol.*, vol. 113, no. 1, pp. 182–191, Jan. 2015.

[7] V. Glaser, A. Holobar, and D. Zazula, "Real-Time Motor Unit Identification From High-Density Surface EMG," *IEEE Trans. Neural Syst. Rehabil. Eng.*, vol. 21, no. 6, pp. 949–958, Nov. 2013.

[8] E. Henneman, "Relation between size of neurons and their susceptibility to discharge," *Science*, vol. 126, no. 3287, pp. 1345–1347, Dec. 1957.

[9] A. Holobar and D. Zazula, "Multichannel Blind Source Separation Using Convolution Kernel Compensation," *IEEE Trans. Signal Process.*, vol. 55, no. 9, pp. 4487–4496, Sep. 2007.

[10] A. Holobar and D. Farina, "Blind source identification from the multichannel surface electromyogram," *Physiol. Meas.*, vol. 35, no. 7, pp. R143–R165, Jul. 2014.

[11] A. Holobar, M. A. Minetto, and D. Farina, "Accurate identification of motor unit discharge patterns from high-density surface EMG and validation with a novel signal-based performance metric," *J Neural Eng.*, vol. 11, no. 1, p. 016008, Feb. 2014.

[12] A. Hyvärinen. Fast and Robust Fixed-Point Algorithms for Independent Component Analysis. IEEE Transactions on Neural Networks 10(3):626-634, 1999

[13] C. G. Kukulka and H. P. Clamann, "Comparison of the recruitment and discharge properties of motor units in human brachial biceps and adductor pollicis during isometric contractions," *Brain Res.*, vol. 219, no. 1, pp. 45–55, Aug. 1981.

[14] A. Del Vecchio, F. Negro, A. Holobar, A. Casolo, J. P. Folland, F. Felici, D. Farina: You are as fast as your motor neurons: speed of recruitment and maximal discharge of motor neurons determine the maximal rate of force development in humans, The Journal of Physiology, vol. 597, no. 9, pp. 2445-2456.